Laboratoire de Traitement de l'Information Médicale
Laboratory of Medical Information Processing

La science pour la santé
From science to health

Université de Bretagne Occidentale

# Joint PET/CT Reconstruction Using a Double Variational Autoencoder

Noel Jeffrey Pinton[1], Alexandre Bousse[1], Catherine Cheze-Le-Rest[1,2], and Dimitris Visvikis[1]

[1]LaTIM, INSERM UMR 1101, Université de Bretagne Occidentale, 29238 Brest, France
[2]CHU Poitiers, Poitiers, France

08 November 2023

# Overview

Introduction

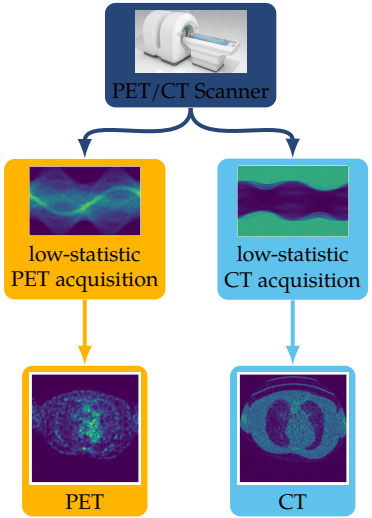
Methodology

Results

Conclusion and Future Work

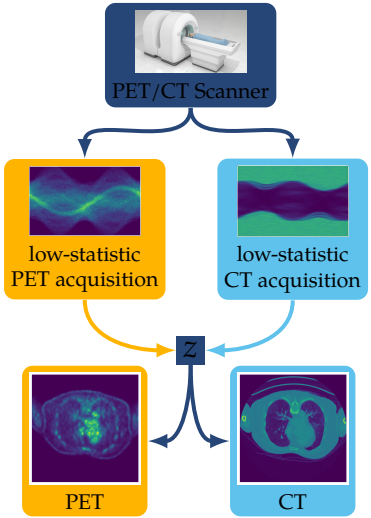
Bibliography

# PET and CT Reconstruction



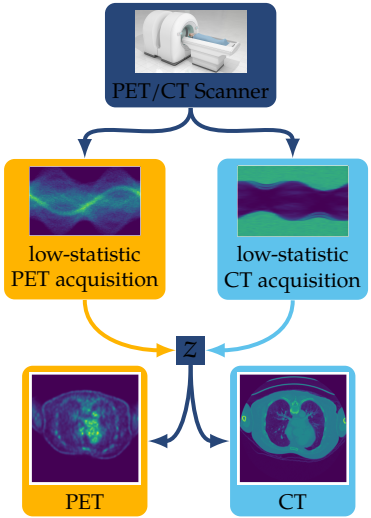

- Standard PET/CT reconstruction: Each modality is reconstructed individually

# PET and CT Reconstruction




- Standard PET/CT reconstruction: Each modality is reconstructed individually
- Joint reconstruction: take advantage of inter-modal information
- Sharing information ➔ noise reduction
- Noise reduction ➔ patient dose reduction
- Shared information must be learned ➔ machine learning

# PET and CT Reconstruction




- Standard PET/CT reconstruction: Each modality is reconstructed individually
- Joint reconstruction: take advantage of inter-modal information
- Sharing information ➔ noise reduction
- Noise reduction ➔ patient dose reduction
- Shared information must be learned ➔ machine learning
- Proposed work: learned penalty for joint reconstruction of PET and CT

# Conventional PET/CT Iterative Reconstruction

- Two images to reconstruct $\boldsymbol{\lambda}$ (PET), $\boldsymbol{\mu}$ (CT):

$$\hat{\boldsymbol{\lambda}} = \arg\min_{\boldsymbol{\lambda}} L_{\text{PET}}(\boldsymbol{\lambda}) + \alpha R_{\text{PET}}(\boldsymbol{\lambda})$$

$$\hat{\boldsymbol{\mu}} = \arg\min_{\boldsymbol{\mu}} L_{\text{CT}}(\boldsymbol{\mu}) + \beta R_{\text{CT}}(\boldsymbol{\mu})$$

# Conventional PET/CT Iterative Reconstruction

- Two images to reconstruct $\boldsymbol{\lambda}$ (PET), $\boldsymbol{\mu}$ (CT):

$$\hat{\boldsymbol{\lambda}} = \arg\min_{\boldsymbol{\lambda}} L_{\text{PET}}(\boldsymbol{\lambda}) + \alpha R_{\text{PET}}(\boldsymbol{\lambda})$$

$$\hat{\boldsymbol{\mu}} = \arg\min_{\boldsymbol{\mu}} L_{\text{CT}}(\boldsymbol{\mu}) + \beta R_{\text{CT}}(\boldsymbol{\mu})$$

- PET: penalized EM (PEM) [De Pierro 1995]
- CT: Penalized weighted least-squares (PWLS) [Elbakri and Fessler 2002]

# Joint PET/CT Reconstruction

- Two images to reconstruct $\boldsymbol{\lambda}$ (PET), $\boldsymbol{\mu}$ (CT):

$$(\hat{\boldsymbol{\lambda}}, \hat{\boldsymbol{\mu}}) \in L_{\text{PET}}(\boldsymbol{\lambda}) + L_{\text{CT}}(\boldsymbol{\mu}) + \gamma R_{\text{syn}}(\boldsymbol{\lambda}, \boldsymbol{\mu})$$

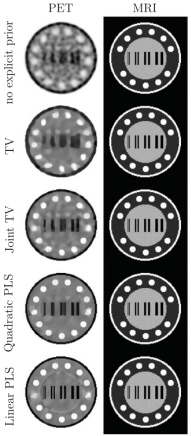



Figure: Joint PET/MRI recon. with JTV and PLS [Ehrhardt et al. 2014]

# Joint PET/CT Reconstruction

- Two images to reconstruct $\boldsymbol{\lambda}$ (PET), $\boldsymbol{\mu}$ (CT):

$$(\hat{\boldsymbol{\lambda}}, \hat{\boldsymbol{\mu}}) \in L_{\text{PET}}(\boldsymbol{\lambda}) + L_{\text{CT}}(\boldsymbol{\mu}) + \gamma R_{\text{syn}}(\boldsymbol{\lambda}, \boldsymbol{\mu})$$

- Joint Total Variation (JTV) [Sapiro and Ringach 1996; Blomgren and Chan 1998]:

$$R_{\text{syn}}(\boldsymbol{\lambda}, \boldsymbol{\mu}) = \sum_j \sqrt{\|\nabla_j \boldsymbol{\lambda}\|^2 + \|\nabla_j \boldsymbol{\mu}\|^2}$$

→ promotes joint sparsity of the gradient

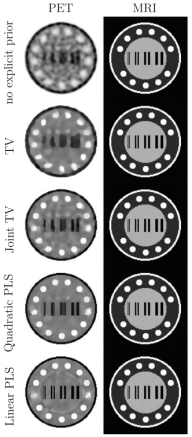



Figure: Joint PET/MRI recon. with JTV and PLS [Ehrhardt et al. 2014]

# Joint PET/CT Reconstruction

- Two images to reconstruct $\lambda$ (PET), $\mu$ (CT):

$$(\hat{\lambda}, \hat{\mu}) \in L_{\text{PET}}(\lambda) + L_{\text{CT}}(\mu) + \gamma R_{\text{syn}}(\lambda, \mu)$$

- Joint Total Variation (JTV) [Sapiro and Ringach 1996; Blomgren and Chan 1998]:

$$R_{\text{syn}}(\lambda, \mu) = \sum_j \sqrt{\|\nabla_j \lambda\|^2 + \|\nabla_j \mu\|^2}$$

→ promotes joint sparsity of the gradient

- Alternatives: Generalized JTV [Mehranian et al. 2017], nuclear TV [Lefkimmiatis et al. 2013; Rigie and La Rivière 2015], parallel levelsets [Ehrhardt et al. 2014], syn-net[Corda-D'Incan et al. 2020]

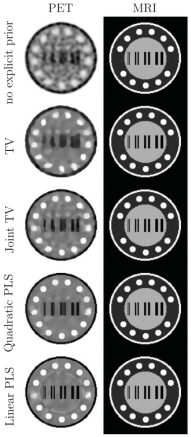



Figure: Joint PET/MRI recon. with JTV and PLS [Ehrhardt et al. 2014]

# Learned Joint PET/CT Reconstruction

- Coupled Dictionary Learning [Sudarshan, Chen, et al. 2018; Sudarshan, Egan, et al. 2020]

$$\boldsymbol{D}_1^*, \boldsymbol{D}_2^* = \underset{\boldsymbol{D}_1, \boldsymbol{D}_2 \in C}{\arg\min} \min_{\{\boldsymbol{z}_{l,p}\}} \sum_l \sum_p \gamma_1 \|\boldsymbol{P}_p \boldsymbol{\lambda}_l - \boldsymbol{D}_1 \boldsymbol{z}_{l,p}\|^2 + \gamma_2 \|\boldsymbol{P}_p \boldsymbol{\mu}_l - \boldsymbol{D}_2 \boldsymbol{z}_{l,p}\|^2 + \|\boldsymbol{z}_{l,p}\|_q, \quad q = 0, 1$$

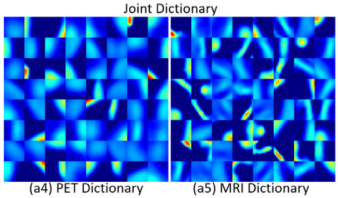



Figure: Coupled PET/MRI dict. learn. [Sudarshan, Egan, et al. 2020]

# Learned Joint PET/CT Reconstruction

- Coupled Dictionary Learning [Sudarshan, Chen, et al. 2018; Sudarshan, Egan, et al. 2020]

$$\boldsymbol{D}_1^*, \boldsymbol{D}_2^* = \underset{\boldsymbol{D}_1, \boldsymbol{D}_2 \in C}{\arg\min} \min_{\{\boldsymbol{z}_{l,p}\}} \sum_l \sum_p \gamma_1 \|\boldsymbol{P}_p \boldsymbol{\lambda}_l - \boldsymbol{D}_1 \boldsymbol{z}_{l,p}\|^2 + \gamma_2 \|\boldsymbol{P}_p \boldsymbol{\mu}_l - \boldsymbol{D}_2 \boldsymbol{z}_{l,p}\|^2 + \|\boldsymbol{z}_{l,p}\|_q, \quad q = 0, 1$$

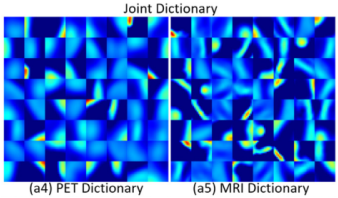



Figure: Coupled PET/MRI dict. learn. [Sudarshan, Egan, et al. 2020]

- Synergistic penalty:

$$R_{\text{syn}}(\boldsymbol{\lambda}, \boldsymbol{\mu}) = \min_{\{\boldsymbol{z}_{l,p}\}} \sum_p \gamma_1 \|\boldsymbol{P}_p \boldsymbol{\lambda} - \boldsymbol{D}_1 \boldsymbol{z}_p\|^2 + \gamma_2 \|\boldsymbol{P}_p \boldsymbol{\mu} - \boldsymbol{D}_2 \boldsymbol{z}_p\|^2 + \|\boldsymbol{z}_p\|_q,$$

# Learned Joint PET/CT Reconstruction

- Coupled Dictionary Learning [Sudarshan, Chen, et al. 2018; Sudarshan, Egan, et al. 2020]

$$\boldsymbol{D}_1^*, \boldsymbol{D}_2^* = \underset{\boldsymbol{D}_1, \boldsymbol{D}_2 \in C}{\arg\min} \min_{\{\boldsymbol{z}_{l,p}\}} \sum_l \sum_p \gamma_1 \|\boldsymbol{P}_p \boldsymbol{\lambda}_l - \boldsymbol{D}_1 \boldsymbol{z}_{l,p}\|^2 + \gamma_2 \|\boldsymbol{P}_p \boldsymbol{\mu}_l - \boldsymbol{D}_2 \boldsymbol{z}_{l,p}\|^2 + \|\boldsymbol{z}_{l,p}\|_q, \quad q = 0, 1$$

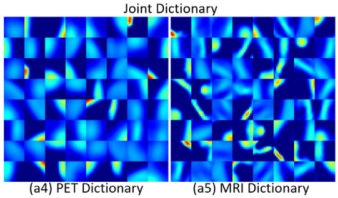



Figure: Coupled PET/MRI dict. learn. [Sudarshan, Egan, et al. 2020]

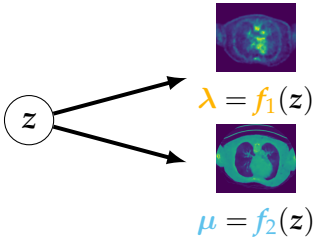
- Synergistic penalty:

$$R_{\text{syn}}(\boldsymbol{\lambda}, \boldsymbol{\mu}) = \min_{\{\boldsymbol{z}_{l,p}\}} \sum_p \gamma_1 \|\boldsymbol{P}_p \boldsymbol{\lambda} - \boldsymbol{D}_1 \boldsymbol{z}_p\|^2 + \gamma_2 \|\boldsymbol{P}_p \boldsymbol{\mu} - \boldsymbol{D}_2 \boldsymbol{z}_p\|^2 + \|\boldsymbol{z}_p\|_q,$$

- Requires extracting many overlapping patches for shift invariance

# Proposed Approach: Double Generative Model

- Replacing the sparse code $z$ by a latent variable, and the dictionaries $D_1$ and $D_2$ by 2 neural networks $f_1$ and $f_2$

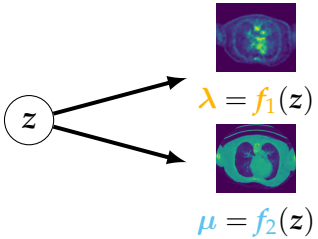


# Proposed Approach: Double Generative Model

- Replacing the sparse code $z$ by a latent variable, and the dictionaries $\boldsymbol{D}_1$ and $\boldsymbol{D}_2$ by 2 neural networks $f_1$ and $f_2$
- Proposed synergistic penalty

$$R_{\text{syn}}(\boldsymbol{\lambda}, \boldsymbol{\mu}) = \min_{z} \eta \|\boldsymbol{\lambda} - f_1(z)\|^2 + (1-\eta)\|\boldsymbol{\mu} - f_2(z)\|^2$$

- $R_{\text{syn}}(\boldsymbol{\lambda}, \boldsymbol{\mu}) \approx 0$ if $\boldsymbol{\lambda}$ and $\boldsymbol{\mu}$ originates from the same $z$



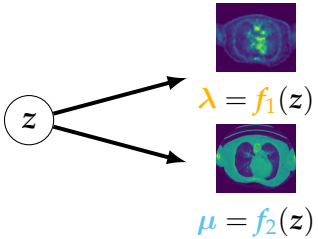
# Proposed Approach: Double Generative Model

- Replacing the sparse code $z$ by a latent variable, and the dictionaries $D_1$ and $D_2$ by 2 neural networks $f_1$ and $f_2$
- Proposed synergistic penalty

$$R_{\text{syn}}(\lambda, \mu) = \min_{z} \eta \|\lambda - f_1(z)\|^2 + (1-\eta)\|\mu - f_2(z)\|^2$$

- $R_{\text{syn}}(\lambda, \mu) \approx 0$ if $\lambda$ and $\mu$ originates from the same $z$
- $\eta$ balances the weight of each modality
- Joint reconstruction:

$$\hat{\lambda}, \hat{\mu} \in \arg\min_{\lambda, \mu} L_{\text{PET}}(\lambda) + L_{\text{CT}}(\mu) + \gamma R_{\text{syn}}(\lambda, \mu)$$



# Overview

Introduction

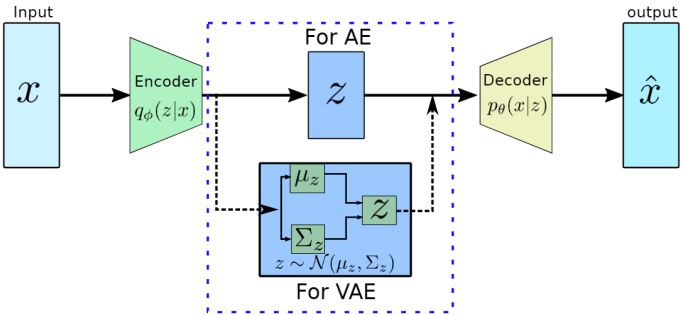
Methodology

Results

Conclusion and Future Work

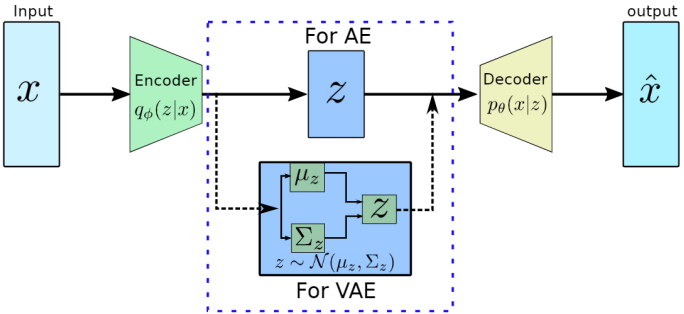
Bibliography

# Variational Auto-encoder



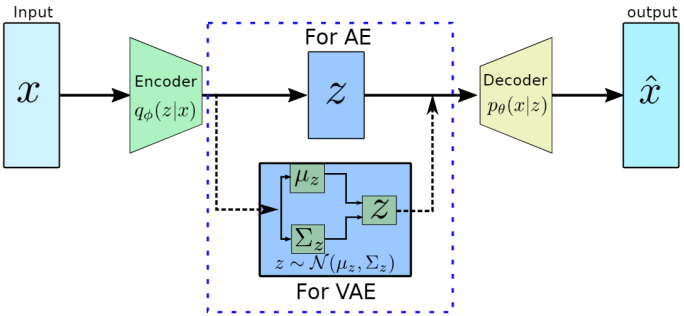

- The encoder compresses input data into a lower-dimensional latent space

# Variational Auto-encoder



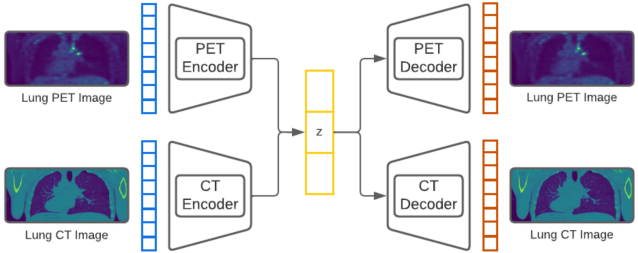

- The encoder compresses input data into a lower-dimensional latent space
- The latent space is a continuous space representation of the input data

# Variational Auto-encoder



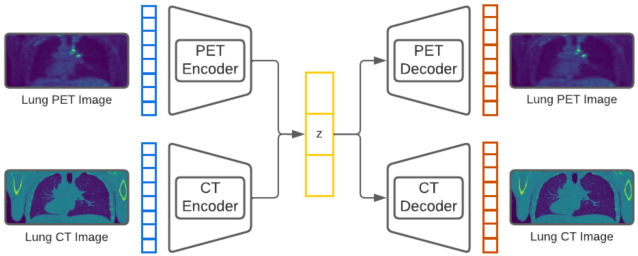

- The encoder compresses input data into a lower-dimensional latent space
- The latent space is a continuous space representation of the input data
- Unsupervised learning; doesn't require paired data

# Multi-branch beta-VAE



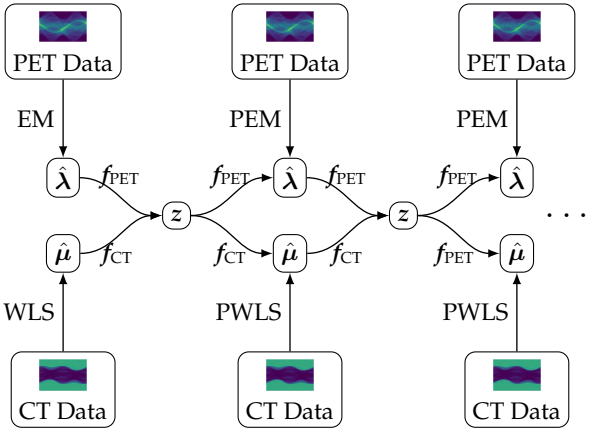

- PET and CT images have their own encoder and decoder pair
- They only share information in the latent space
- The encoder outputs are concatenated before the latent space

# Multi-branch beta-VAE




- Multibranch networks can use different branches to extract features at different scales, orientations, and locations [Zhang et al. 2018]
- Multibranch networks can learn more diverse and complex features by using different types of layers and operations in each branch.

# Synergistic PET/CT Reconstruction Algorithm




initialization

$\boldsymbol{p} = \boldsymbol{P}^\top \mathbf{1}; \boldsymbol{b} = -\log \boldsymbol{y}/h$

Initialize $\hat{\boldsymbol{\lambda}}$ and $\hat{\boldsymbol{\mu}}$ by EM and WLS

For $k = 1$: `OuterIter`

$\boldsymbol{z}^k = \arg\min_z \ \eta \|\boldsymbol{f}_{\text{PET}}(\boldsymbol{z}) - \hat{\boldsymbol{\lambda}}\|^2 + (1-\eta)\|\boldsymbol{f}_{\text{CT}}(\boldsymbol{z}) - \hat{\boldsymbol{\mu}}\|^2$

$\boldsymbol{c} \leftarrow \gamma\eta \boldsymbol{f}_{\text{PET}}(\boldsymbol{z}^n) - \boldsymbol{p}$

For $l = 1$: `SubIter1`

$\hat{\boldsymbol{\lambda}}^{\text{em}} \leftarrow \hat{\boldsymbol{\lambda}} \frac{1}{\boldsymbol{p}} \boldsymbol{P}^\top \left[\frac{\boldsymbol{g}}{\boldsymbol{P}\hat{\boldsymbol{\lambda}}}\right]$

$\hat{\boldsymbol{\lambda}} \leftarrow \frac{\boldsymbol{c} + \sqrt{\boldsymbol{c}^2 + 4\gamma\eta\boldsymbol{p}\hat{\boldsymbol{\lambda}}^{\text{em}}}}{2\gamma\eta}$

end For

For $m = 1$: `SubIter2`

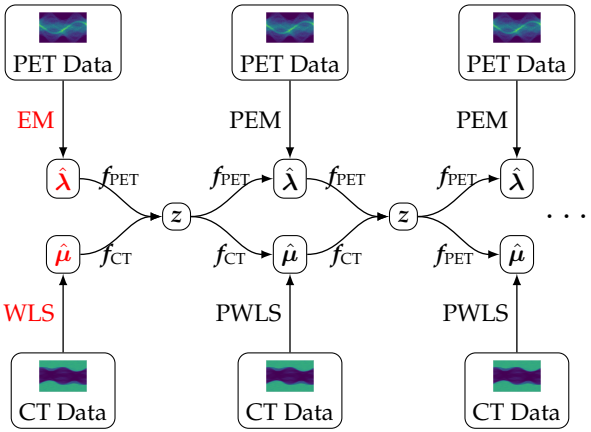
$\hat{\boldsymbol{\mu}}^{\text{rec}} \leftarrow \hat{\boldsymbol{\mu}} - \boldsymbol{D}^{-1}\boldsymbol{A}^\top \boldsymbol{W}(\boldsymbol{A}\hat{\boldsymbol{\mu}} - \boldsymbol{b})$

$\hat{\boldsymbol{\mu}} \leftarrow \left[\frac{\boldsymbol{D}\hat{\boldsymbol{\mu}}^{\text{rec}} + \gamma(1-\eta)\boldsymbol{f}_{\text{CT}}(\boldsymbol{z}^n)}{\boldsymbol{D} + \gamma(1-\eta)}\right]_+$

end For

end For

# Synergistic PET/CT Reconstruction Algorithm




initialization

$\boldsymbol{p} = \boldsymbol{P}^\top \mathbf{1}; \boldsymbol{b} = -\log \boldsymbol{y}/h$

Initialize $\hat{\boldsymbol{\lambda}}$ and $\hat{\boldsymbol{\mu}}$ by EM and WLS

For $k = 1$: `OuterIter`

$\boldsymbol{z}^k = \arg\min_z \ \eta \|f_{\text{PET}}(\boldsymbol{z}) - \hat{\boldsymbol{\lambda}}\|^2 + (1-\eta)\|f_{\text{CT}}(\boldsymbol{z}) - \hat{\boldsymbol{\mu}}\|^2$

$\boldsymbol{c} \leftarrow \gamma\eta f_{\text{PET}}(\boldsymbol{z}^n) - \boldsymbol{p}$

For $l = 1$: `SubIter1`

$\hat{\boldsymbol{\lambda}}^{\text{em}} \leftarrow \hat{\boldsymbol{\lambda}} \frac{1}{\boldsymbol{p}} \boldsymbol{P}^\top \left[\frac{\boldsymbol{g}}{\boldsymbol{P}\hat{\boldsymbol{\lambda}}}\right]$

$\hat{\boldsymbol{\lambda}} \leftarrow \frac{\boldsymbol{c} + \sqrt{\boldsymbol{c}^2 + 4\gamma\eta\boldsymbol{p}\hat{\boldsymbol{\lambda}}^{\text{em}}}}{2\gamma\eta}$

end For

For $m = 1$: `SubIter2`

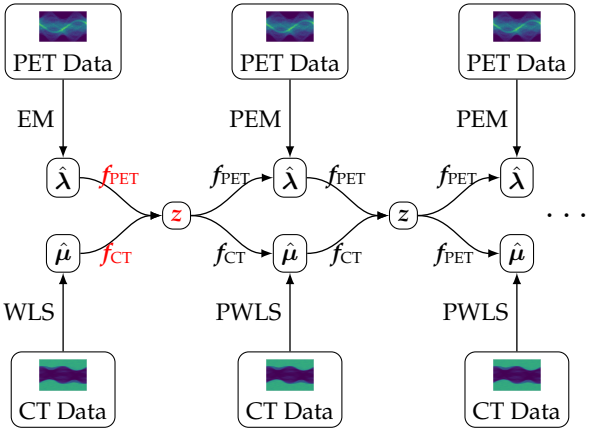
$\hat{\boldsymbol{\mu}}^{\text{rec}} \leftarrow \hat{\boldsymbol{\mu}} - \boldsymbol{D}^{-1}\boldsymbol{A}^\top \boldsymbol{W}(\boldsymbol{A}\hat{\boldsymbol{\mu}} - \boldsymbol{b})$

$\hat{\boldsymbol{\mu}} \leftarrow \left[\frac{\boldsymbol{D}\hat{\boldsymbol{\mu}}^{\text{rec}} + \gamma(1-\eta)f_{\text{CT}}(\boldsymbol{z}^n)}{\boldsymbol{D} + \gamma(1-\eta)}\right]_+$

end For

end For

# Synergistic PET/CT Reconstruction Algorithm




initialization

$\boldsymbol{p} = \boldsymbol{P}^\top \mathbf{1}; \boldsymbol{b} = -\log \boldsymbol{y}/h$

Initialize $\hat{\boldsymbol{\lambda}}$ and $\hat{\boldsymbol{\mu}}$ by EM and WLS

For $k = 1$: `OuterIter`

$\boldsymbol{z}^k = \arg\min_{\boldsymbol{z}} \eta \|f_{\text{PET}}(\boldsymbol{z}) - \hat{\boldsymbol{\lambda}}\|^2 + (1-\eta)\|f_{\text{CT}}(\boldsymbol{z}) - \hat{\boldsymbol{\mu}}\|^2$

$\boldsymbol{c} \leftarrow \gamma\eta f_{\text{PET}}(\boldsymbol{z}^n) - \boldsymbol{p}$

For $l = 1$: `SubIter1`

$\hat{\boldsymbol{\lambda}}^{\text{em}} \leftarrow \hat{\boldsymbol{\lambda}} \frac{1}{\boldsymbol{p}} \boldsymbol{P}^\top \left[\frac{\boldsymbol{g}}{\boldsymbol{P}\hat{\boldsymbol{\lambda}}}\right]$

$\hat{\boldsymbol{\lambda}} \leftarrow \frac{\boldsymbol{c} + \sqrt{\boldsymbol{c}^2 + 4\gamma\eta\boldsymbol{p}\hat{\boldsymbol{\lambda}}^{\text{em}}}}{2\gamma\eta}$

end For

For $m = 1$: `SubIter2`

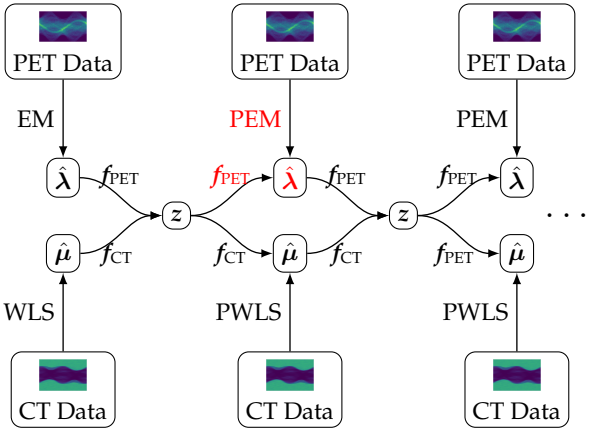
$\hat{\boldsymbol{\mu}}^{\text{rec}} \leftarrow \hat{\boldsymbol{\mu}} - \boldsymbol{D}^{-1}\boldsymbol{A}^\top \boldsymbol{W}(\boldsymbol{A}\hat{\boldsymbol{\mu}} - \boldsymbol{b})$

$\hat{\boldsymbol{\mu}} \leftarrow \left[\frac{\boldsymbol{D}\hat{\boldsymbol{\mu}}^{\text{rec}} + \gamma(1-\eta)f_{\text{CT}}(\boldsymbol{z}^n)}{\boldsymbol{D} + \gamma(1-\eta)}\right]_+$

end For

end For

# Synergistic PET/CT Reconstruction Algorithm




initialization

$\boldsymbol{p} = \boldsymbol{P}^\top \mathbf{1}; \boldsymbol{b} = -\log \boldsymbol{y}/h$

Initialize $\hat{\boldsymbol{\lambda}}$ and $\hat{\boldsymbol{\mu}}$ by EM and WLS

For $k = 1$: `OuterIter`

$\boldsymbol{z}^k = \arg\min_{\boldsymbol{z}} \eta \|f_{\text{PET}}(\boldsymbol{z}) - \hat{\boldsymbol{\lambda}}\|^2 + (1-\eta)\|f_{\text{CT}}(\boldsymbol{z}) - \hat{\boldsymbol{\mu}}\|^2$

$\boldsymbol{c} \leftarrow \gamma\eta f_{\text{PET}}(\boldsymbol{z}^n) - \boldsymbol{p}$

For $l = 1$: `SubIter1`

$\hat{\boldsymbol{\lambda}}^{\text{em}} \leftarrow \hat{\boldsymbol{\lambda}} \frac{1}{\boldsymbol{p}} \boldsymbol{P}^\top \left[\frac{\boldsymbol{g}}{\boldsymbol{P}\hat{\boldsymbol{\lambda}}}\right]$

$\hat{\boldsymbol{\lambda}} \leftarrow \frac{\boldsymbol{c} + \sqrt{\boldsymbol{c}^2 + 4\gamma\eta\boldsymbol{p}\hat{\boldsymbol{\lambda}}^{\text{em}}}}{2\gamma\eta}$

end For

For $m = 1$: `SubIter2`

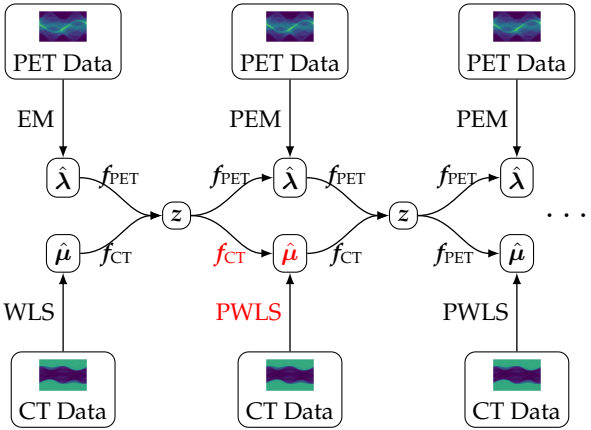
$\hat{\boldsymbol{\mu}}^{\text{rec}} \leftarrow \hat{\boldsymbol{\mu}} - \boldsymbol{D}^{-1}\boldsymbol{A}^\top \boldsymbol{W}(\boldsymbol{A}\hat{\boldsymbol{\mu}} - \boldsymbol{b})$

$\hat{\boldsymbol{\mu}} \leftarrow \left[\frac{\boldsymbol{D}\hat{\boldsymbol{\mu}}^{\text{rec}} + \gamma(1-\eta)f_{\text{CT}}(\boldsymbol{z}^n)}{\boldsymbol{D} + \gamma(1-\eta)}\right]_+$

end For

end For

# Synergistic PET/CT Reconstruction Algorithm




initialization

$\boldsymbol{p} = \boldsymbol{P}^\top \mathbf{1}; \boldsymbol{b} = -\log \boldsymbol{y}/h$

Initialize $\hat{\boldsymbol{\lambda}}$ and $\hat{\boldsymbol{\mu}}$ by EM and WLS

For $k = 1$: `OuterIter`

$\boldsymbol{z}^k = \arg\min_z \ \eta \|f_{\text{PET}}(z) - \hat{\boldsymbol{\lambda}}\|^2 + (1-\eta)\|f_{\text{CT}}(z) - \hat{\boldsymbol{\mu}}\|^2$

$\boldsymbol{c} \leftarrow \gamma\eta f_{\text{PET}}(\boldsymbol{z}^n) - \boldsymbol{p}$

For $l = 1$: `SubIter1`

$\hat{\boldsymbol{\lambda}}^{\text{em}} \leftarrow \hat{\boldsymbol{\lambda}} \frac{1}{\boldsymbol{p}} \boldsymbol{P}^\top \left[\frac{\boldsymbol{g}}{\boldsymbol{P}\hat{\boldsymbol{\lambda}}}\right]$

$\hat{\boldsymbol{\lambda}} \leftarrow \frac{c + \sqrt{c^2 + 4\gamma\eta\boldsymbol{p}\hat{\boldsymbol{\lambda}}^{\text{em}}}}{2\gamma\eta}$

end For

For $m = 1$: `SubIter2`

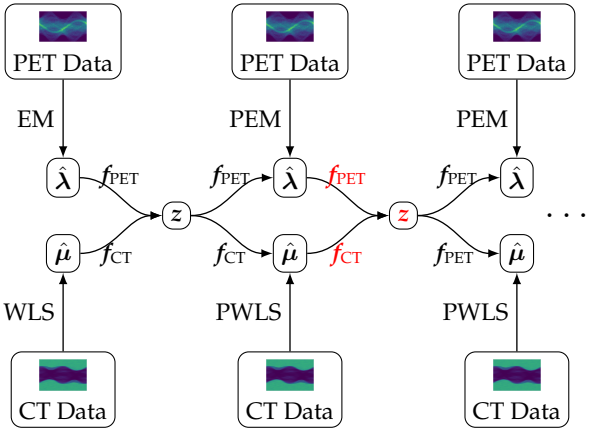
$\hat{\boldsymbol{\mu}}^{\text{rec}} \leftarrow \hat{\boldsymbol{\mu}} - \boldsymbol{D}^{-1}\boldsymbol{A}^\top \boldsymbol{W}(\boldsymbol{A}\hat{\boldsymbol{\mu}} - \boldsymbol{b})$

$\hat{\boldsymbol{\mu}} \leftarrow \left[\frac{\boldsymbol{D}\hat{\boldsymbol{\mu}}^{\text{rec}} + \gamma(1-\eta) f_{\text{CT}}(\boldsymbol{z}^n)}{\boldsymbol{D} + \gamma(1-\eta)}\right]_+$

end For

end For

# Synergistic PET/CT Reconstruction Algorithm




initialization

$\boldsymbol{p} = \boldsymbol{P}^\top \mathbf{1}; \boldsymbol{b} = -\log \boldsymbol{y}/h$

Initialize $\hat{\boldsymbol{\lambda}}$ and $\hat{\boldsymbol{\mu}}$ by EM and WLS

For $k = 1$: `OuterIter`

$\boldsymbol{z}^k = \arg\min_{\boldsymbol{z}} \eta \|\boldsymbol{f}_{\text{PET}}(\boldsymbol{z}) - \hat{\boldsymbol{\lambda}}\|^2 + (1-\eta)\|\boldsymbol{f}_{\text{CT}}(\boldsymbol{z}) - \hat{\boldsymbol{\mu}}\|^2$

$\boldsymbol{c} \leftarrow \gamma\eta \boldsymbol{f}_{\text{PET}}(\boldsymbol{z}^n) - \boldsymbol{p}$

For $l = 1$: `SubIter1`

$\hat{\boldsymbol{\lambda}}^{\text{em}} \leftarrow \hat{\boldsymbol{\lambda}} \frac{1}{\boldsymbol{p}} \boldsymbol{P}^\top \left[\frac{\boldsymbol{g}}{\boldsymbol{P}\hat{\boldsymbol{\lambda}}}\right]$

$\hat{\boldsymbol{\lambda}} \leftarrow \frac{\boldsymbol{c} + \sqrt{\boldsymbol{c}^2 + 4\gamma\eta\boldsymbol{p}\hat{\boldsymbol{\lambda}}^{\text{em}}}}{2\gamma\eta}$

end For

For $m = 1$: `SubIter2`

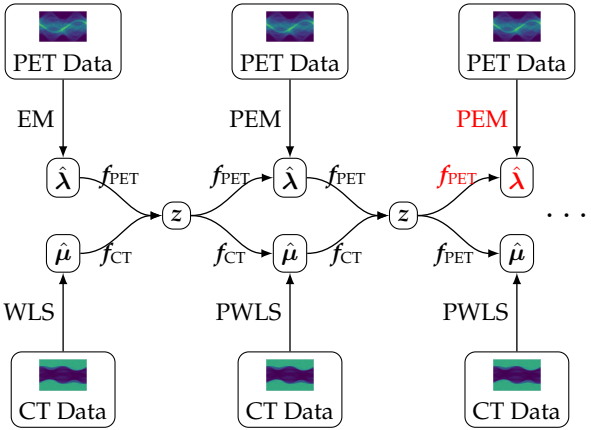
$\hat{\boldsymbol{\mu}}^{\text{rec}} \leftarrow \hat{\boldsymbol{\mu}} - \boldsymbol{D}^{-1}\boldsymbol{A}^\top \boldsymbol{W}(\boldsymbol{A}\hat{\boldsymbol{\mu}} - \boldsymbol{b})$

$\hat{\boldsymbol{\mu}} \leftarrow \left[\frac{\boldsymbol{D}\hat{\boldsymbol{\mu}}^{\text{rec}} + \gamma(1-\eta)\boldsymbol{f}_{\text{CT}}(\boldsymbol{z}^n)}{\boldsymbol{D} + \gamma(1-\eta)}\right]_+$

end For

end For

# Synergistic PET/CT Reconstruction Algorithm




initialization

$\boldsymbol{p} = \boldsymbol{P}^\top \mathbf{1}; \boldsymbol{b} = -\log \boldsymbol{y}/h$

Initialize $\hat{\boldsymbol{\lambda}}$ and $\hat{\boldsymbol{\mu}}$ by EM and WLS

For $k = 1$: `OuterIter`

$\boldsymbol{z}^k = \arg\min_z \ \eta\|f_{\text{PET}}(z) - \hat{\boldsymbol{\lambda}}\|^2 + (1-\eta)\|f_{\text{CT}}(z) - \hat{\boldsymbol{\mu}}\|^2$

$\boldsymbol{c} \leftarrow \gamma\eta f_{\text{PET}}(\boldsymbol{z}^n) - \boldsymbol{p}$

For $l = 1$: `SubIter1`

$\hat{\boldsymbol{\lambda}}^{\text{em}} \leftarrow \hat{\boldsymbol{\lambda}} \frac{1}{\boldsymbol{p}} \boldsymbol{P}^\top \left[\frac{\boldsymbol{g}}{\boldsymbol{P}\hat{\boldsymbol{\lambda}}}\right]$

$\hat{\boldsymbol{\lambda}} \leftarrow \frac{\boldsymbol{c} + \sqrt{\boldsymbol{c}^2 + 4\gamma\eta\boldsymbol{p}\hat{\boldsymbol{\lambda}}^{\text{em}}}}{2\gamma\eta}$

end For

For $m = 1$: `SubIter2`

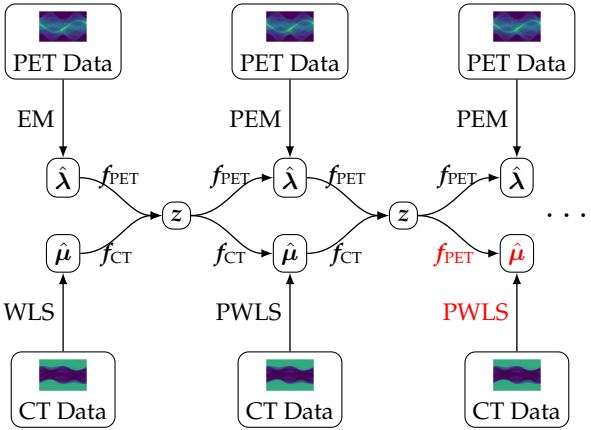
$\hat{\boldsymbol{\mu}}^{\text{rec}} \leftarrow \hat{\boldsymbol{\mu}} - \boldsymbol{D}^{-1}\boldsymbol{A}^\top \boldsymbol{W}(\boldsymbol{A}\hat{\boldsymbol{\mu}} - \boldsymbol{b})$

$\hat{\boldsymbol{\mu}} \leftarrow \left[\frac{\boldsymbol{D}\hat{\boldsymbol{\mu}}^{\text{rec}} + \gamma(1-\eta)f_{\text{CT}}(\boldsymbol{z}^n)}{\boldsymbol{D} + \gamma(1-\eta)}\right]_+$

end For

end For

# Synergistic PET/CT Reconstruction Algorithm




initialization

$\boldsymbol{p} = \boldsymbol{P}^\top \mathbf{1}; \boldsymbol{b} = -\log \boldsymbol{y}/h$

Initialize $\hat{\boldsymbol{\lambda}}$ and $\hat{\boldsymbol{\mu}}$ by EM and WLS

For $k = 1$: `OuterIter`

$\boldsymbol{z}^k = \arg\min_z \ \eta \|f_{\text{PET}}(z) - \hat{\boldsymbol{\lambda}}\|^2 + (1-\eta)\|f_{\text{CT}}(z) - \hat{\boldsymbol{\mu}}\|^2$

$\boldsymbol{c} \leftarrow \gamma\eta f_{\text{PET}}(\boldsymbol{z}^n) - \boldsymbol{p}$

For $l = 1$: `SubIter1`

$\hat{\boldsymbol{\lambda}}^{\text{em}} \leftarrow \hat{\boldsymbol{\lambda}} \frac{1}{\boldsymbol{p}} \boldsymbol{P}^\top \left[\frac{\boldsymbol{g}}{\boldsymbol{P}\hat{\boldsymbol{\lambda}}}\right]$

$\hat{\boldsymbol{\lambda}} \leftarrow \frac{\boldsymbol{c} + \sqrt{\boldsymbol{c}^2 + 4\gamma\eta\boldsymbol{p}\hat{\boldsymbol{\lambda}}^{\text{em}}}}{2\gamma\eta}$

end For

For $m = 1$: `SubIter2`

$\hat{\boldsymbol{\mu}}^{\text{rec}} \leftarrow \hat{\boldsymbol{\mu}} - \boldsymbol{D}^{-1}\boldsymbol{A}^\top \boldsymbol{W}(\boldsymbol{A}\hat{\boldsymbol{\mu}} - \boldsymbol{b})$

$\hat{\boldsymbol{\mu}} \leftarrow \left[\frac{\boldsymbol{D}\hat{\boldsymbol{\mu}}^{\text{rec}} + \gamma(1-\eta) f_{\text{CT}}(\boldsymbol{z}^n)}{\boldsymbol{D} + \gamma(1-\eta)}\right]_+$

end For

end For

# Overview

Introduction

Methodology

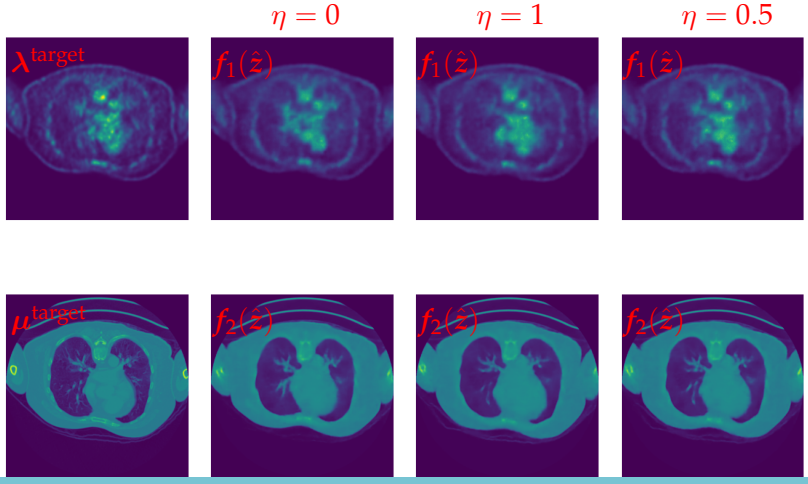
Results

Conclusion and Future Work

Bibliography

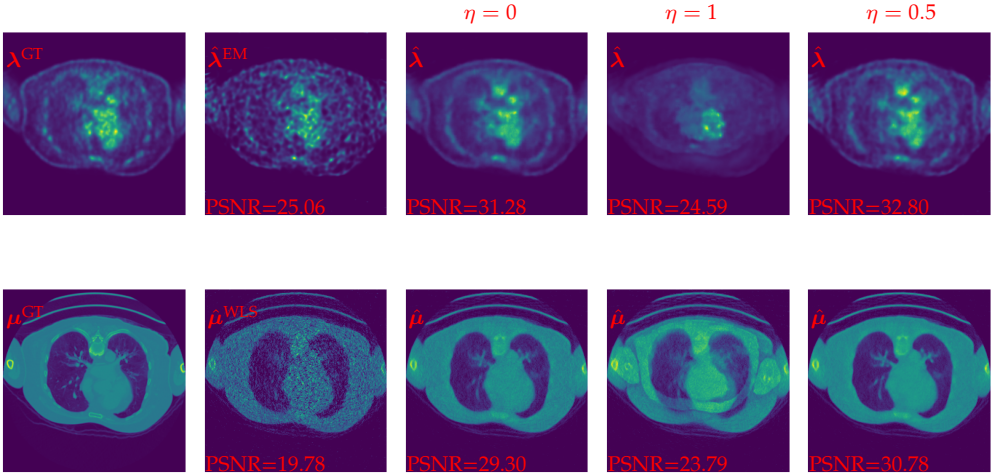
# Generated Images by fitting $z$

$$\hat{z} = \arg\min_z \ \eta\|\lambda^{\text{target}} - f_1(z)\|^2 + (1-\eta)\|\mu^{\text{target}} - f_2(z)\|^2$$



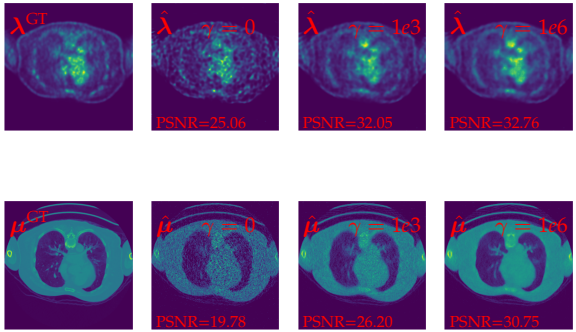
# Joint PET/CT Reconstruction

- $(\hat{\lambda}, \hat{\mu}) \in L_{\text{PET}}(\lambda) + L_{\text{CT}}(\mu) + \gamma R_{\text{syn}}(\lambda, \mu)$, $R_{\text{syn}}(\lambda, \mu) = \min_z \eta\|\lambda - f_1(z)\|^2 + (1-\eta)\|\mu - f_2(z)\|^2$.
- PET and CT projection data generated from $\boldsymbol{\lambda}^{\text{GT}}$ and $\boldsymbol{\mu}^{\text{GT}}$



# Effect of the Generative Model

$$\hat{\lambda}, \hat{\mu} \in \arg\min_{\lambda,\mu} L_{\text{PET}}(\lambda) + L_{\text{CT}}(\mu) + \gamma R_{\text{syn}}(\lambda, \mu)$$



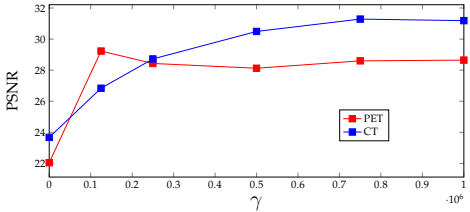
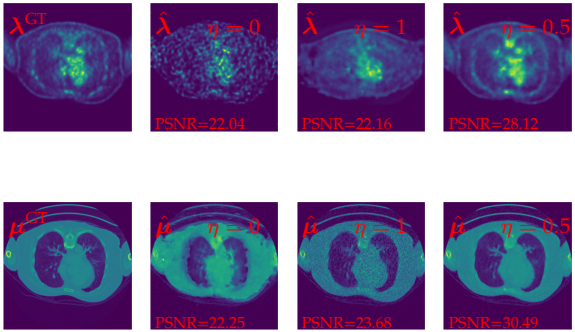




Figure: PSNR values of reconstructed PET/CT images with respect to $\gamma$ at $\eta = 0.5$.

# Effect of Inter-modality Information

$$R_{\text{syn}}(\lambda, \mu) = \min_z \ \eta\|\lambda - f_1(z)\|^2 + (1-\eta)\|\mu - f_2(z)\|^2$$



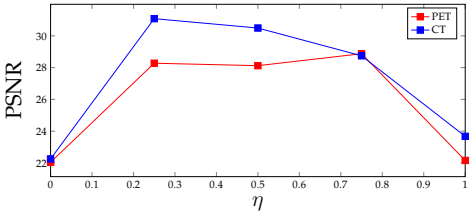
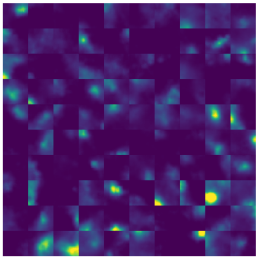
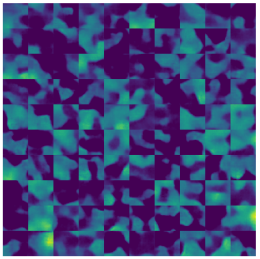




Figure: PSNR values of reconstructed PET/CT images with respect to $\eta$ at $\gamma = 5 \times 10^5$.

# Patch-based Joint Image Reconstruction v1



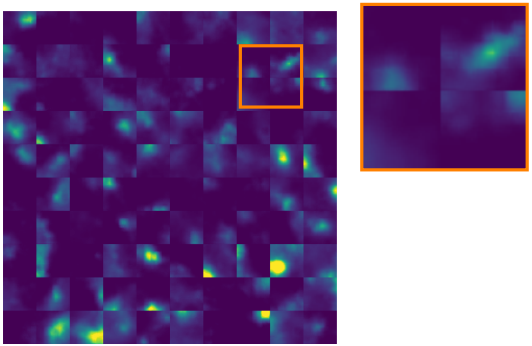
$\lambda^{\text{patches}}$



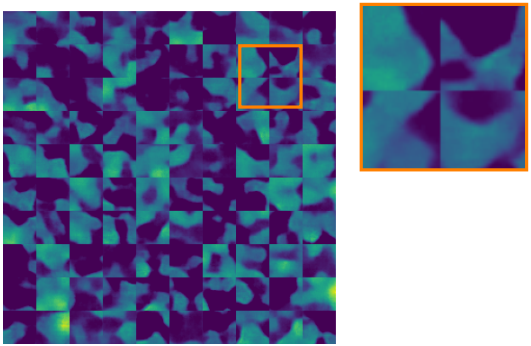
$\mu^{\text{patches}}$

- Generated patches from random $z$ values to the PET and CT decoder
- Patches are trained from 32 $x$ 32 patches extracted from 512 $x$ 512 paired PET and CT images

# Patch-based Joint Image Reconstruction v2



$\lambda$patches



$\mu$patches

# Patch-based Joint Reconstruction Algorithm

$\boldsymbol{p} = \boldsymbol{P}^\top \mathbf{1}; \boldsymbol{b} = -\log \boldsymbol{y}/h$

Initialize $\hat{\boldsymbol{\lambda}}$ and $\hat{\boldsymbol{\mu}}$ by EM and WLS

For $k = 1$: `OuterIter`

$\boldsymbol{Z} = \arg\min_{\boldsymbol{Z}} \eta\|\boldsymbol{E}\hat{\boldsymbol{\lambda}} - f_1(\boldsymbol{Z})\|^2 + (1-\eta)\|\boldsymbol{E}\hat{\boldsymbol{\mu}} - f_2(\boldsymbol{Z})\|^2$

$\hat{\boldsymbol{\lambda}}^{\text{reg}} = \hat{\boldsymbol{\lambda}}^{\text{reg}} - \boldsymbol{D}_2^{-1}\boldsymbol{E}^\top(\boldsymbol{E}\hat{\boldsymbol{\lambda}}^{\text{reg}} - f_1(\boldsymbol{Z}))$

$\hat{\boldsymbol{\mu}}^{\text{reg}} = \hat{\boldsymbol{\mu}}^{\text{reg}} - \boldsymbol{D}_2^{-1}\boldsymbol{E}^\top(\boldsymbol{E}\hat{\boldsymbol{\mu}}^{\text{reg}} - f_2(\boldsymbol{Z}))$

$\boldsymbol{c} \leftarrow \gamma\eta\hat{\boldsymbol{\lambda}}^{\text{reg}} - \boldsymbol{p}$

For $l = 1$: `SubIter1`

$\hat{\boldsymbol{\lambda}}^{\text{em}} \leftarrow \hat{\boldsymbol{\lambda}}\frac{1}{p}\boldsymbol{P}^\top\left[\frac{g}{\boldsymbol{P}\hat{\boldsymbol{\lambda}}}\right]$

$\hat{\boldsymbol{\lambda}} \leftarrow \frac{c+\sqrt{c^2+4\gamma\eta p\boldsymbol{\lambda}^{\text{em}}}}{2\gamma\eta}$

end For

For $m = 1$: `SubIter2`

$\hat{\boldsymbol{\mu}}^{\text{rec}} \leftarrow \hat{\boldsymbol{\mu}} - \boldsymbol{D}^{-1}\boldsymbol{A}^\top\boldsymbol{W}(\boldsymbol{A}\hat{\boldsymbol{\mu}} - \boldsymbol{b})$

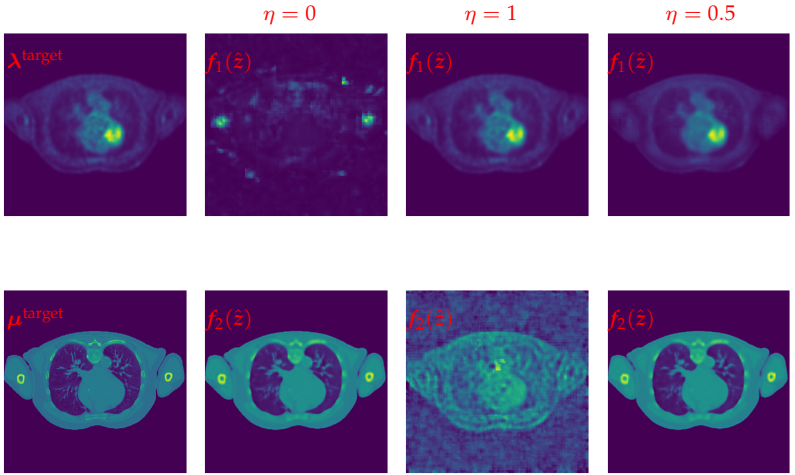
$\hat{\boldsymbol{\mu}} \leftarrow \left[\frac{D\hat{\boldsymbol{\mu}}^{\text{rec}}+\gamma(1-\eta)\hat{\boldsymbol{\mu}}^{\text{reg}}}{D+\gamma(1-\eta)}\right]_+$

end For

end For

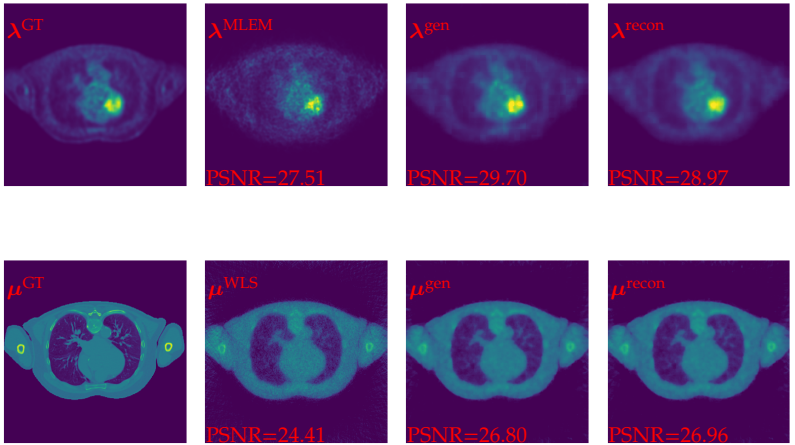
# Generated Images by fitting $z$

$$Z = \arg\min_Z \ \eta \|E\lambda - f_1(Z)\|^2 + \ (1-\eta)\|E\mu - f_2(Z)\|^2$$



# Patch-based Synergistic Reconstruction

- $(\hat{\boldsymbol{\lambda}}, \hat{\boldsymbol{\mu}}) \in L_{\text{PET}}(\boldsymbol{\lambda}) + L_{\text{CT}}(\boldsymbol{\mu}) + \gamma R_{\text{syn}}(\boldsymbol{\lambda}, \boldsymbol{\mu}), \quad R_{\text{syn}}(\boldsymbol{\lambda}, \boldsymbol{\mu}) = \min_{\boldsymbol{Z}} \eta \|\boldsymbol{E}\boldsymbol{\lambda} - f_1(\boldsymbol{Z})\|^2 + (1-\eta)\|\boldsymbol{E}\boldsymbol{\mu} - f_2(\boldsymbol{Z})\|^2.$
- PET and CT projection data generated from $\boldsymbol{\lambda}^{\text{GT}}$ and $\boldsymbol{\mu}^{\text{GT}}$



# Overview

Introduction

Methodology

Results

Conclusion and Future Work

Bibliography

# Conclusion

- We trained a multi-branch VAE to generate paired PET/CT images, improving image quality.

# Conclusion

- We trained a multi-branch VAE to generate paired PET/CT images, improving image quality.
- The results demonstrated significant improvements in both modalities, indicating mutual enhancement.

# Conclusion

- We trained a multi-branch VAE to generate paired PET/CT images, improving image quality.
- The results demonstrated significant improvements in both modalities, indicating mutual enhancement.
- Future research should explore other generative techniques and validate them on larger datasets.

# Acknowledgment





Laboratoire de Traitement de l'Information Médicale
Laboratory of Medical Information Processing



Inserm
La science pour la santé
From science to health

anr

UBO
Université de Bretagne Occidentale

- This work is funded by the French National Research Agency (ANR) with grant number ANR-20-CE45-0020.
- CHU Poitiers for the PET and CT Images
- Collaborators from CREATIS and BioMaps

cnrs

CHU Poitiers

CREATIS

BioMaps
Laboratoire d'Imagerie Biomédicale

cea

# Overview

Introduction

Methodology

Results

Conclusion and Future Work

Bibliography

# Bibliography I




P. Blomgren and T. F. Chan. “Color TV: total variation methods for restoration of vector-valued images”. In: *IEEE transactions on image processing* 7.3 (1998), pp. 304–309.



G. Corda-D’Incan, J. A. Schnabel, and A. J. Reader. “Syn-Net for Synergistic Deep-Learned PET-MR Reconstruction”. In: *2020 IEEE Nuclear Science Symposium and Medical Imaging Conference (NSS/MIC)*. 2020, pp. 1–5. DOI: 10.1109/NSS/MIC42677.2020.9508086.



A. R. De Pierro. “A modified expectation maximization algorithm for penalized likelihood estimation in emission tomography”. In: *IEEE transactions on medical imaging* 14.1 (1995), pp. 132–137.



M. J. Ehrhardt, K. Thielemans, L. Pizarro, D. Atkinson, S. Ourselin, B. F. Hutton, and S. R. Arridge. “Joint reconstruction of PET-MRI by exploiting structural similarity”. In: *Inverse Problems* 31.1 (2014), p. 015001.



I. A. Elbakri and J. A. Fessler. “Statistical image reconstruction for polyenergetic X-ray computed tomography”. In: *IEEE transactions on medical imaging* 21.2 (2002), pp. 89–99.



S. Lefkimmiatis, A. Roussos, M. Unser, and P. Maragos. “Convex generalizations of total variation based on the structure tensor with applications to inverse problems”. In: *International Conference on Scale Space and Variational Methods in Computer Vision*. Springer. 2013, pp. 48–60.

# Bibliography II




A. Mehranian, M. A. Belzunce, C. Prieto, A. Hammers, and A. J. Reader. "Synergistic PET and SENSE MR image reconstruction using joint sparsity regularization". In: *IEEE transactions on medical imaging* 37.1 (2017), pp. 20–34.



D. S. Rigie and P. J. La Rivière. "Joint reconstruction of multi-channel, spectral CT data via constrained total nuclear variation minimization". In: *Physics in Medicine & Biology* 60.5 (2015), p. 1741.



G. Sapiro and D. L. Ringach. "Anisotropic diffusion of multivalued images with applications to color filtering". In: *IEEE transactions on image processing* 5.11 (1996), pp. 1582–1586.



V. P. Sudarshan, Z. Chen, and S. P. Awate. "Joint PET+MRI patch-based dictionary for Bayesian random field PET reconstruction". In: *International Conference on Medical Image Computing and Computer-Assisted Intervention*. Springer. 2018, pp. 338–346.



V. P. Sudarshan, G. F. Egan, Z. Chen, and S. P. Awate. "Joint PET-MRI image reconstruction using a patch-based joint-dictionary prior". In: *Medical image analysis* 62 (2020), p. 101669.



H. Zhang, J. Shao, and R. Salakhutdinov. "Deep Neural Networks with Multi-Branch Architectures Are Less Non-Convex". en. In: arXiv:1806.01845 (June 2018). arXiv:1806.01845 [cs, stat]. URL: http://arxiv.org/abs/1806.01845.

Thank you for listening.